IRF-2 Inhibits Cancer Proliferation by Promoting AMER1 Transcription in Human Gastric Cancer

Yanjie Chen
Zhongshan Hospital Fudan University
Shuneng Luo
Zhongshan Hospital Fudan University
Hao Wu
Zhongshan Hospital Fudan University
Ningping Zhang
Zhongshan Hospital Fudan University
Ling Dong
Zhongshan Hospital Fudan University
Taotao Liu
Zhongshan Hospital Fudan University
Li Liang (liang.li@zs-hospital.sh.cn)
Zhongshan Hospital Fudan University https://orcid.org/0000-0002-1694-380X
Xizhong Shen
Zhongshan Hospital Fudan University

Research Article

Keywords: IRF-2, AMER1, wnt/β-catenin signaling pathway, gastric cancer, prognosis

Posted Date: October 20th, 2021

DOI: https://doi.org/10.21203/rs.3.rs-925869/v1

IRF-2 Inhibits Cancer Proliferation by Promoting AMER1 Transcription in Human Gastric Cancer

Running head: IRF-2 inhibit GC by promoting AMER1 transcription

Author: Yan-Jie Chen[1], Shu-Neng Luo[1], Hao Wu[1], Ning-Ping Zhang[1], Ling Dong[1], Tao-Tao Liu[1], Li Liang[2*], Xi-Zhong Shen[1*]

Author address: [1]Department of Gastroenterology, Zhongshan Hospital of Fudan University, Shanghai 200032, China; [2]Department of Medical Oncology, Zhongshan Hospital, Fudan University, 180 Fenglin Road, Shanghai 200032, China

***Correspondences:** Xi-Zhong Shen, MD, PhD, Department of Gastroenterology, Zhongshan Hospital of Fudan University, 180 Fenglin Rd., Shanghai 200032, China; Tel: +86-21-64041990-2070; Fax: +86-21-64038038; E-mail: shen.xizhong@zs-hospital.sh.cn.

Li Liang, MD, Department of Medical Oncology, Zhongshan Hospital, Fudan University, 180 Fenglin Road, Shanghai 200032, China; E-mail: liang.li@zs-hospital.sh.cn.

Abstract

Interferon regulatory factor 2 (IRF-2) plays the roles of an anti-oncogene in gastric cancer (GC). However, the mechanism remains unknow. The expression of IRF-2 in GC tissues and adjacent non-tumor tissues was found by immunohistochemistry (IHC) and the predictive values of IRF-2 for the prognosis of GC patients were explored. Cell function experiments and xenograft tumor growth in nude mice were performed to test the proliferation ability of the tumor in vitro and in vivo. Chromatin Immunoprecipitation assay (ChIP-Seq) was used to verify the direct target of IRF-2. We found that the IRF-2 expression was down regulated in GC tissues and was negatively correlated with prognosis of GC patients. IRF-2 could negatively affect GC cells proliferation in vitro and in vivo. ChIP-Seq assay showed IRF-2 could directly activate AMER1 transcription and regulate Wnt/β-catenin signaling pathway, which was validated by IHC both in tissue microarray and xenografted tumor tissues, western blot analysis, and cell function experiment. In conclusion, high expression of IRF-2 can inhibit tumor growth and affect the prognosis of patients through inhibiting Wnt/β-catenin signaling pathway by directly regulating AMER1 transcription in GC.

Keywords: IRF-2; AMER1; wnt/β-catenin signaling pathway; gastric cancer; prognosis

ABBREVIATIONS

IRF-2, Interferon regulatory factor 2;

IHC, immunohistochemistry;

ChIP-Seq, Chromatin Immunoprecipitation assay;

GC, Gastric cancer;

HCC, hepatocellular carcinoma;

APC, adenomatous polyposis coli;

AMER1, APC membrane recruitment 1;

GAC, gastric adenocarcinoma;

TNM, tumor-node-metastasis;

UICC, International Union Contra Cancrum;

TMAs, tissue microarrays;

HE, hematoxylin and eosin;

shIRF-2, short hairpin RNA for IRF-2;

EdU, 5-Ethynyl-2′-deoxyuridine;

OS, overall survival time;

DFS, cancer free survival time;

ICI, immune checkpoint inhibitors;

anti-PD-1/L1, anti-programmed death-1/anti-programmed death ligand-1;

anti-CTLA4, anti-cytotoxic T-lymphocyte-associated protein 4;

1 Introduction

Gastric cancer (GC) is ranked as the fifth most frequent malignancies with 1,000,000 new cases in 2018 worldwide [1]. It is estimated that almost 679,100 new cases developed in China each year, making GC the second most deadly form of cancer in China [2]. Although great advances have been made in diagnosis and therapy, the prognosis of advanced GC still remains poor [3]. Therefore, it is crucial to investigate the molecular pathogenesis of GC to predict the prognosis and develop potential therapeutic targets.

The interferon regulatory factor (IRF) family in human is a kind of transcriptional factors which can modify several gene expressions by directly targeting the DNA promoter sequences of target genes [4]. IRF-2 is a crucial member of IRF family, located on chromosome 4q34.1-q35.1, and it has no expression of tissue specificity. It has been found to play critical roles in oncogenesis, cell apoptosis, immune regulation, and cell differentiation. Recurrent alterations of IRF-2 gene were found in hepatocellular carcinoma (HCC) by Zucman-Rossi and his colleagues [5], indicating its key role in the development of tumors. Further studies found that the inactivation of IRF-2 led to impaired P53 function making it a tumor suppressor in HCC [5,6]. Recent research found that IRF-2 could down-regulate PD-L1 promoter activity and protein levels in HCC [7]. Frequent loss of IRF-2 led to decreased MHC class I antigen presentation and increased PD-L1 expression in cancer, and finally resulted in immune evasion [8]. It was also found that KRAS mediated repression of IRF-2, which led to high expression of CXCL3 and low expression of CXCR2. Higher IRF-2 expression led to increased responsiveness to

anti-PD-1 therapy in colorectal cancer [9].

APC (adenomatous polyposis coli) membrane recruitment 1 (AMER1) is a plasma membrane-associated protein which contains 1135 amino acids. It can interact with APC with three binding domains which share no obvious sequence similarity [10]. AMER1 was identified as a tumor suppressor by regulating the Wnt/β-catenin signaling pathway. It can specifically bind phosphatidylinositol 4,5-bisphosphate, translocate to the cell membrane and interact with key regulators of the canonical Wnt/β-catenin signaling pathway, such as components of the β-catenin destruction complex [11,12]. Wnt/β-catenin signaling pathway is one of the key pathways participating in GC development and can regulate various expression of factors which are involved in the differentiation, invasion and metastasis of GC [13]. Inhibition of the Wnt/β-catenin signaling pathway can down regulate the expression of β-catenin, c-myc, and CD44, and decrease the proliferation ability of GC cells [14]. On the other hand, enhance Wnt/β-catenin activity can promote tumor formation and promote stem cell-like features in GC cells [14].

Our previous studies have found that miR-18a could directly target IRF-2 and modulate the expression of IRF-2, thus affecting the expression of P53 and MMP-1 in GC [15,16]. In this study, we found that high expression of IRF-2 can inhibit tumor growth and positively affect the prognosis of patients by directly regulating AMER1 transcription in GC.

2 Materials and Methods

2.1 Patients and Specimens

Tumor specimens were obtained from 72 gastric adenocarcinoma (GAC) who underwent curative resection at Zhongshan Hospital of Fudan University between 2011 and 2014. The inclusion and exclusion criteria are listed as follows: (a) having a distinctive pathologic diagnosis of GAC. (b) having curative gastric surgical treatment with a complete resection of all the cancer nodules. Histological examination shows no tumor cells on the cut surface. (c) having complete follow-up data until June 2017. (d) having suitable formalin-fixed and paraffin-embedded tissues. (e) patient agreeing to participate in the study and sign informed consent. The GAC diagnosis based on WHO criteria and the tumor stage was classified according to the 7th edition of tumor-node-metastasis (TNM) classification of Union for International Cancer Control (UICC). Ethical approval for human subjects was obtained from the research ethics committee of Zhongshan Hospital of Fudan University. The clinical characteristics of all the patients were listed in Table 1.

Most of the patients were treated with systemic chemotherapy or traditional Chinese medicine according to their clinical conditions. After the conclusion of treatment, patients were followed every 6 months; monitored by chest, abdomen and pelvic enhanced CT scanning. The endoscopy exam was performed annually. Patient with confirmed cancer recurrence received further treatment.

2.2 Immunohistochemistry (IHC) and Staining Evaluation

Cancer tissue and adjacent normal tissue were formalin-fixed and paraffin-embedded and made into tissue microarrays (TMAs) after hematoxylin and eosin (HE) staining and histopathology guided location. Five-micron thick sections of TMA were deparaffinized and rehydrated, followed by high-temperature antigen retrieval via microwave in 0.1 M citrate solution (pH 6.0) for 15 minutes. The sections were incubated with mouse anti-IRF-2 antibody (Abcam, Cambridge, UK), anti-FAM123B (Abcam, Cambridge, UK) overnight at 4°C. Then they was incubated for 30 minutes with secondary antibody at room temperature and immunostained by the avidin-biotin complex technique using 3,3'-diaminobenzidine. Hematoxylin was used as a counterstain.

Two pathologists evaluated the immunohistochemical staining respectively. The interpretation of immunoreactivity was calculated by analyzing the extent and intensity of staining positivity of cells: "≤5% cell positivity" or "negative staining" = 0; "6-20% cell positivity" or "light staining" = 1; "21-50% cell positivity" or "mild staining" = 2; ">50% cell positivity" or "intense staining" = 3. Total score is the product of the two. The final score was the score of the adjacent tissue minus the score of the cancer tissue. Greater than 2.5 and 2 were considered low expression in IRF-2 and AMER1 separately, otherwise they were identified as high expression.

2.3 Cell Culture, Transfection and Virus Infection

Human GC cell lines MKN-45 and SGC-7901 were obtained from Cell Bank of Typed Culture Collection of Chinese Academy of Science, Shanghai Institute of Biochemistry

and Cell Biology, Shanghai, China, and cultured in RPMI 1640 medium (HuClone, USA) supplemented with 10% fetal bovine serum (FBS, Corning, USA) at 37°C in an incubator containing 5% CO_2.

For the experiments utilizing overexpression, the IRF-2 full-length sequence was synthesized and subcloned into an expression vector CMV-MCS-3XFlag-PGK-Puro (Genechem, China). MKN45 cells were transfected with CMV-IRF2-3XFlag-PGK-Puro according to manufacturer's instructions. For the knockdown experiments, short hairpin RNA for IRF-2 (shIRF-2) was generated by Genechem (China) and inserted into the pHY-LV-KD1.4 lentiviral shRNA vector (Hanyinbt, China). SGC-7901 cells were transfected with lentiviral shIRF-2 and subjected to selection with puromycin to establish a stable cell line. The stable monoclonal cell lines with up-regulated and down-regulated IRF-2 were screened. The efficacy of overexpression and knockdown of IRF-2 were verified by real-time PCR and western blot.

For the experiments utilizing overexpression, the AMER1 full-length sequence was synthesized and subcloned into a pcDNA3.1 vector (Genechem, China). MKN45 cells were transfected with pcDNA3.1-IRF-2 using Lipofectamine 3000 (Invitrogen, USA) according to manufacturer's instructions. For the knockdown experiments, SGC-7901 cells were transfected with AMER1 siRNA according to manufacturer's instructions (Genechem, China).

2.4 Protein Extraction and Western Blot Analysis

Protein extraction and western blot was performed according to the standard protocols

by antibodies against IRF-2 (Abcam, USA), AMER1 (Abcam, USA), CD44 (EPITMICS, USA), c-myc (Abcam, USA), β-catenin (CST, USA), OCT-4 (Abcam, USA), COX-2 (Abcam, USA). β-actin (Abcam, USA) was selected as a loading control.

2.5 Real-time PCR

Total RNA was extracted from the cells and tissues using the TRIzol™ Reagent (Invitrogen) according to the manufacturer's instructions. A total of 0.5 μg RNA from each sample was subjected to reverse transcription to obtain cDNA using a SuperScript™ III First-Strand Synthesis System Kit (Thermo Fisher Scientific). The resulting cDNA was diluted 100-fold and applied to a Real-time PCR (RT-PCR) assay using a Real-time PCR System (Applied Biosystems, USA) with a SYBR Green PCR Master Mix kit (TaKaRa, Japan) following the protocols. The $2^{-\Delta\Delta Ct}$ method was used to analyze the relative fold changes. The experiments were carried out in triplicate for each data point.

The AMER1 primers used for PCR were 5'- GGGCTGGACCCCACTGT -3′ (forward) and 5’-CTGCTCAACAGCATCTATCG-3′ (reverse); while the IRF2 primers used for PCR were 5’- CGAATGCTGCCCCTATCAGA -3’ (forward) and 5’-TCCTACAACTATGATGTTCACCGT -3’ (reverse). The GAPDH was used as an internal control and was detected using the following primers: 5’-AATCCCATCACCATCTTCC-3′ (forward) and 5’-AGTCCTTCCACGACCAA-3′ (reverse).

2.6 Detection of Cell Proliferation

Plate colony formation assay and 5-Ethynyl-2′-deoxyuridine (EdU) assay were conducted according to the standard protocols. Briefly, with respect to plate colony formation assay, 500 cells/well were seeded in 6-well plate. The cells were mixed and then cultured for 2 weeks in culture medium with 10% FBS. Clusters containing more than 30 cells were counted as a single colony. Cell-Light™ EdU Apollo®488 In Vitro Imaging Kit (RiboBio, China) was used to measure cell proliferation. Images of cells were obtained by Nikon microscope (Nikon, Japan). All experiments were repeated three times

2.7 ChIP-seq

Twenty million OE-IRF2-MKN45 cells were grown and washed, and then crosslinked with 1% formaldehyde for 10 minutes at room temperature. Crosslinking was quenched by addition of glycine to a final concentration of 0.15 M for 5 min at room temperature. Crosslinked cells were washed with ice-cold PBS, the supernatant was discarded, and the pellets were flash-frozen in liquid nitrogen and stored at -80 °C.

For each sample, 20 million fixed cells were lysed to prepare nuclear extracts. After chromatin shearing by sonication, lysates were incubated overnight at 4°C with protein A Dynabeads coupled with 5 μg of antibody. After immunoprecipitation, beads were recovered using a magnet and washed. DNA was eluted and cross links reverted at 65 ° C for 4 hours then purified with QIAGEN Kit. DNA was quantitated using the Qubit® dsDNA HS assay and a Qubit® 2.0 Fluorimeter (Invitrogen). For ChIP-Seq, 5ng of purified ChIP DNA were used to generate the sequencing library using a NEB kit and

sequenced with the Illumina HiSeq X Ten. Each sample was tested at least three times. For ChIP-seq data analysis, FastQC software was used to evaluate the quality of the original data. The original data were then compared to the reference genome using BWA or Bowtie2 software. MACS was used for peak calling, genome location annotation of peak mining, motif analysis of peaks area, and GO and KEGG enrichment analysis of the target genes.

2.8 Luciferase Assay

Then the AMER1-wild and -mut were inserted into the pGL3 promoter vector (GenScript Co., Ltd., Nanjing, China) which was transfected into 7901 and MKN-45 cells using Lipofectamine 2000 (Invitrogen: Thermo Fisher Scientific, Inc.) along with IRF2 overexpression vector or NC vectors. Cells were seeded in the 24-well plates. 48 h later, firefly luciferase signals and renilla luciferase (internal reference) were detected by a dual-luciferase reporter assay kit (Promega, Madison, WI, USA.) referring to the manufacture's protocols. All experiments were repeated in triplicate.

2.9 Xenograft Tumor Growth in Nude Mice

Ten female BALB/c nude mice that were 4 to 6 weeks old and 18 to 20 g in weight, were obtained from Shanghai Experimental Animal Center (Shanghai, China). shIRF2-SGC7901 cells and NC-SGC7901 cells (2×10^6) were harvested and injected subcutaneously into the nude mice (five mice per group). Tumor growth was quantified every 2 days after tumor formation and tumor volumes were calculated by length × width^2 × 0.5. The mice were sacrificed, and the tumors were taken out 23 days later.

Tumor tissues were formalin-fixed, paraffin-embedded, HE stained, and immunohistochemical stained to measure the expression level of IRF-2, AMER1, and CD44. All xenograft experiments were approved by the Animal Experiments Ethics Committee of Zhongshan Hospital of Fudan University.

2.10 Statistical Analyses

Statistical analyses were done by SPSS 26.0 (SPSS Inc., IL, USA) and GraphPad Prism 7 (GraphPad Software, Inc., CA, USA). Mann-Whitney test, Student's t test, paired t test, $\chi 2$ test, and Fisher's exact probability were used for comparison between groups. Kaplan-Meier method and log-rank test were used to calculate cumulative survival time. The prognostic value of IRF-2 was measured by Univariate and multivariate analyses based on the Cox proportional hazard regression model. All tests were two-sided. $P < 0.05$ was regarded as statistically significant.

3 Results

3.1 The IRF-2 Expression is Downregulated in GC Tissues and Related with Prognosis

It was found that IRF-2 was mostly located in cytoplasm and downregulated in human GC tissues compare with the normal adjacent tissues ($P < 0.001$; Fig. 1A, B) by immunohistochemically analyses. The average score of IRF-2 is 3.90 ± 1.56 in GC tissues, while 6.35 ± 1.65 in normal adjacent tissues.

In order to find the relationship between the expression level of IRF-2 and clinical characteristics of the GC patients, we collected the patients' data and summarized it in Table 1. There is no correlation between the expression of IRF-2 and clinical characteristics including age, sex, tumor size, invasive depth, lymph nodes metastasis, tumor position, and TNM stage ($P > 0.05$).

Kaplan-Meier analysis and log-rank test were used to evaluate the influence of IRF-2 on survival. We found that IRF-2 expression level was significantly positively correlated with patients' overall survival time (OS) ($P < 0.001$, Fig. 1C) and cancer free survival time (DFS) ($P = 0.014$, Fig. 1D), which means higher IRF-2 expression correlated with longer DFS and OS. It was found that tumor size, TNM stage, invasive depth, and lymph nodes metastasis were unfavorable predictors for OS; and that tumor size, TNM stage, invasive depth, lymph nodes metastasis, and distant metastases were unfavorable predictors for DFS, while IRF-2 was a favorable factor for OS and DFS of GC (Table 2). Considering the invasive depth, lymph nodes metastasis, and distant

metastases were included in the TNM stage, we only bring the tumor size, TNM stage, and expression of IRF-2 into the multivariate analysis. It was found that IRF-2 was an independent prognosticator for OS ($P < 0.001$) and DFS ($P = 0.002$) in this analysis.

3.2 IRF-2 Affects Proliferation of Gastric Cancer Cell

The stable cell lines of MKN-45 and SGC-7901 that overexpress and knock down IRF-2 have been constructed and validated in our previous studies [16]. Colony formation assays showed that colony formation ability decreased following IRF-2 overexpressed in MKN-45 cells while it increased following IRF-2 knockdown in SGC-7901cells (Fig. 2A). Similarly, EdU assays also showed that IRF-2 overexpression could inhibit GC cell proliferation while its knockdown could promote GC cell proliferation (Fig. 2B). We further explored whether IRF-2 could affect GC growth in vivo. SGC-7901 cells stably transfected with sh-IRF-2 and empty vector were injected into the nude mice. Twenty-three days after the injection, tumors from the sh-IRF-2 group were significantly bigger than the control group (Fig. 2C). All these findings include indications that IRF-2 can negatively affect GC cells proliferation in vitro and in vivo.

3.3 IRF-2 Directly Activate AMER1 Transcription and Regulate Wnt/β-catenin signaling Pathway

We applied ChIP-Seq to investigate the potential target and binding sites of IRF-2 in GC and found 18565 peaks (Fig. 3A). GO and KEGG enrichment analysis of target genes were used to explore the signaling pathways that IRF-2 may affect. The ten pathways that IRF-2 most affected by GO analysis included tumor necrosis factor-

mediated signaling pathway and the Wnt/β-catenin signaling pathway, which were related to tumor development and progression (Fig. 3B). KEGG analysis also showed that IRF-2 might affect several cancer pathways (Fig. 3C). Combined with the results of microarray assays that we have reported before [16], we found that IRF-2 can inhibits the Wnt/β-catenin signaling pathway by directly targeting the AMER1 transcription start domain. It was found that IRF-2 may act on the promoter region of AMER1 to promote transcription by Chip-Seq (Fig. 3D). Possible binding sites of IRF-2 was found by JASPAR 2020 database (Fig. 3E) [17] and there were two predicted binding sites in the AMER1 transcription start domain (Fig. 3F), which consistent with our ChIP-Seq results. To determine if IRF-2 bound to the AMER1 promoter, we performed luciferase assays. The results showed that IRF-2 can significantly upregulate the luciferase activity of AMER1-promoter-WT, but not AMER1-promoter-Mut1 and AMER1-promoter-Mut2 (Figure 3G), which suggested that IRF-2 binds to the AMER1 promoter in GC.

3.4 IRF-2 Promotes the Expression of AMER1

We verified the expression of AMER1 and the key factors of the Wnt/β-catenin signaling pathway, include CD44, c-myc, β-catenin in lentivirus-infected cell lines. It was found that AMER1 expression increased after IRF-2 was overexpressed; while AMER1 expression decreased when IRF-2 was downregulated both in protein level and mRNA level (Fig. 4A and B). IRF-2 expression was also negatively related with the indexes of stem cell-like features including OCT-4, SOX-2, CD44, and c-myc (Fig.

4A). To further evaluate the relationship between IRF-2 and AMER1 in GAC patients and xenografted tumor tissues in nude mice, we examine the expression levels of AMER1 by immunohistochemical assay using anti-AMER1 antibody in the same TMA specimens and xenografted tumor tissues. Immunohistochemical scores showed a positive correlation between AMER1 and IRF-2 score both in TMA specimens ($r = 0.58$, $P < 0.001$; Fig. 4C) and xenografted tumor tissues ($r = 0.59$, $P < 0.001$; Fig. 4D), while a significant inverse correlation was also found between the expression of AMER1 and CD44 ($r = -1.55$, $P = 0.009$; Fig. 4D). A positive correlation was also found between the expression of IRF-2 and AMER1 on website GEPIA ($r = 0.19$, $P < 0.001$; Fig. 4E).

3.5 IRF-2 Inhibiting the Wnt/β-catenin signaling Pathway Depends on the Regulation of AMER1

To find out if IRF-2 regulate the expression of Wnt/β-catenin signaling pathway by targeting AMER1, we knocked down the expression of AMER1 in MKN-45 cells with or without overexpressed IRF-2. We found that with the downregulation of AMER1, the key molecules in the Wnt/β-catenin signaling pathway and stem cell-like features was upregulated correspondingly, which was independent of the expression of IRF-2 (Fig. 5A). Similar results were also found in the in vitro experiment. Knocking down the expression of AMER1 leaded increased colony formation ability (Fig. 5B) and promoted GC cell proliferation (Fig. 5C) even though IRF-2 was overexpressed. Similarly, inhibition of the Wnt/β-catenin signaling pathway was observed when

AMER1 was upregulated regardless the expression of IRF-2 both in western blot analyses and cytofunctional experiments (Fig. 5D-F). All of the results indicated that the ability of IRF-2 inhibiting the Wnt/β-catenin signaling pathway depended on the regulation of AMER1.

4 Discussion

GC is a common malignancy with a large proportion of cases reported in East Asia. Although clinical diagnosis and treatment techniques are improving, the prognosis of gastric cancer still remains poor. Five-year survival rates remain at about 18% [1]. Therefore, it is very important to screen and study molecules which can predict GC patients' prognosis. In this study, we confirmed in clinical samples that IRF-2 expression is low in GC tissue than in normal tissues and its expression is correlated with prognosis. The expression level of IRF-2 is an independent risk factor for prognosis of GC patients. This part of the results is consisting with our previous study results [16].

The role of IRF-2 in tumors is still controversial in the literature. Some studies found that IRF-2 promotes cancer, while others found the opposite, suggesting that IRF-2 may play multiple regulatory roles in tumors [18]. It was found in our previous studies that IRF-2, which regulated by miR-18a, might function as a tumor suppressor by affecting the expression of P53 and MMP-1 in GC [15,16]. In this study, we found that IRF-2 could directly target and upregulate the transcription of AMER1, which was known as a component of the destruction complex and could interact directly with β-catenin through the C-terminal half. Decrease the expression of AMER1 in mammalian cells stabilizes cellular β-catenin levels and increase the downstream genes of the Wnt/β-catenin signaling pathway [19]. In our study, upregulated IRF-2 expression could increase the expression of AMER1 and inhibit the expression of β-catenin and downstream

molecules (CD44 and c-myc) of the Wnt/β-catenin signaling pathway, while downregulated the expression of IRF-2 led to the opposite trend. Blocking down the expression of AMER1 led to the stability of β-catenin levels and increasing of downstream genes (CD44 and c-myc) of the Wnt/β-catenin signaling pathway. These results indicated that IRF-2 adversely affected the Wnt/β-catenin signaling pathway by regulating AMER1 expression (Supplemental Fig.1).

Currently, immune checkpoint inhibitors (ICI) are widely used in the clinical treatment of various tumors, including anti-programmed death-1/anti-programmed death ligand-1 (anti-PD-1/L1), and anti-cytotoxic T-lymphocyte-associated protein 4 (anti-CTLA4). It was found that IRF-2 could modulate the immunity of tumor cells by down-regulating PD-L1 promoter activity [7], increasing MHC class I antigen presentation and decreasing PD-L1 expression in cancer [8], and leading to increased responsiveness to anti-PD-1 therapy [9], which suggested that IRF-2 plays a role in inhibiting tumor growth not only by transcribing tumor suppressor genes, but also by regulating tumor immunity. Previous studies had identified the Wnt/β-catenin pathway as one of the key oncogenic pathway signals related to immune evasion [20,21]. The expression of β-catenin in the tumor might inverse correlated with $CD8^+$ T cell infiltration [22]. For cancer not responding to ICI treatment like GC, it may possible that inhibitors of Wnt/ β-catenin signaling, such as IRF-2 and AMER1, could improve $CD8^+$ T cell infiltration, and thus produce a more favorable scenario to ICI and become possible adjuvants to ICI. This direction is worth further study in the future.

In this research, we also examined some of the indexes related to stem cell-like features, including OCT-44, SOX-2, CD-44, and c-myc. We found that these indexes were upregulated when IRF-2 was knocked down, indicating that down regulating the expression of IRF-2 might also related with increase of stem cell-like features in GC. But the specific mechanism remains to be further studied.

In conclusion, we found that IRF-2 expression was lower in GC tissue than in normal tissues and that its expression was correlated with prognosis. The expression level of IRF-2 was an independent risk factor for prognosis of GC patients. Decreasing the expression of IRF-2 would enhance the proliferation ability of GC cells both in vitro and in vivo, while upregulated IRF-2 expression led to the opposite results. The results of ChIP-seq, bioinformatics analysis, and western blot showed that IRF-2 could inhibit the Wnt/β-catenin pathway by directly targeting the promoter sequences of AMER1 and enhancing its transcription. Additionally, it was also found that down regulating IRF-2 expression might also be related to the increase of stem cell-like features in GC.

Ethics approval and consent to participate

Ethical approval for human subjects was obtained from the research ethics committee of Zhongshan Hospital of Fudan University. All the patients agreed to participate the study.

Consent for publication

All the authors consent for publication.

Competing interests

The authors declare that there are no conflicts of interest.

Funding

This study was supported by National Natural Science Foundation of China (No. 81900482), Science and Technology Commission of Shanghai Municipality (No. 21ZR1412500), Foundation of Shanghai Municipal Population and Family Planning Commission (No.20174Y0151), Key Basic Research Program of Science and Technology Commission of Shanghai Municipality (No. 20JC1415300).

Authors' contributions

Yan-Jie Chen conceived and designed the experiments; Yan-Jie Chen, Shu-Neng Luo and Hao Wu performed the in vitro and in vivo experiments; Ling Dong and Tao-Tao Liu enrolled and followed-up of patients; Yan-Jie Chen, Li Liang and Xi-Zhong Shen wrote and edited the manuscript.

Acknowledgements

This study was also supported by the project of Innovative Research Team of High-level Local Universities in Shanghai-Clinical and Basic Research on the Prevention and Treatment of Some Inflammatory Diseases by Integrative Medicine.

Availability of data and material

The data that support the findings of this study are included in the main body of the manuscript and supplemental data.

References

1. Bray F, Ferlay J, Soerjomataram I, Siegel RL, Torre LA, Jemal A. Global cancer statistics 2018: GLOBOCAN estimates of incidence and mortality worldwide for 36 cancers in 185 countries. *CA Cancer J Clin*. 2018;68:394-424.

2. Zong L, Abe M, Seto Y, Ji J. The challenge of screening for early gastric cancer in China. *Lancet*. 2016;388:2606.

3. Van Cutsem E, Sagaert X, Topal B, Haustermans K, Prenen H. Gastric cancer. *Lancet*. 2016;388:2654-2664.

4. Zhang R, Chen K, Peng L, Xiong H. Regulation of T helper cell differentiation by interferon regulatory factor family members. *Immunol Res*. 2012;54:169-76.

5. Guichard C, Amaddeo G, Imbeaud S, et al. Integrated analysis of somatic mutations and focal copy-number changes identifies key genes and pathways in hepatocellular carcinoma. *Nat Genet*. 2012;44:694-8.

6. Amaddeo G, Guichard C, Imbeaud S, Zucman-Rossi J. Next-generation sequencing identified new oncogenes and tumor suppressor genes in human hepatic tumors. *Oncoimmunology*. 2012;1:1612-1613.

7. Yan Y, Zheng L, Du Q, Yan B, Geller DA. Interferon regulatory factor 1 (IRF-1) and IRF-2 regulate PD-L1 expression in hepatocellular carcinoma (HCC) cells. *Cancer Immunol Immunother*. 2020;69:1891-1903.

8. Kriegsman BA, Vangala P, Chen BJ, et al. Frequent Loss of IRF2 in Cancers Leads to Immune Evasion through Decreased MHC Class I Antigen

Presentation and Increased PD-L1 Expression. *J Immunol*. 2019;203:1999-2010.

9. Liao W, Overman MJ, Boutin AT, et al. KRAS-IRF2 Axis Drives Immune Suppression and Immune Therapy Resistance in Colorectal Cancer. *Cancer Cell*. 2019;35:559-572 e7.

10. Grohmann A, Tanneberger K, Alzner A, Schneikert J, Behrens J. AMER1 regulates the distribution of the tumor suppressor APC between microtubules and the plasma membrane. *J Cell Sci*. 2007;120:3738-47.

11. Tanneberger K, Pfister AS, Brauburger K, et al. Amer1/WTX couples Wnt-induced formation of PtdIns(4,5)P2 to LRP6 phosphorylation. *EMBO J*. 2011;30:1433-43.

12. Tanneberger K, Pfister AS, Kriz V, Bryja V, Schambony A, Behrens J. Structural and functional characterization of the Wnt inhibitor APC membrane recruitment 1 (Amer1). *J Biol Chem*. 2011;286:19204-14.

13. Wu WK, Cho CH, Lee CW, et al. Dysregulation of cellular signaling in gastric cancer. *Cancer Lett*. 2010;295:144-53.

14. Cai C, Zhu X. The Wnt/beta-catenin pathway regulates self-renewal of cancer stem-like cells in human gastric cancer. *Mol Med Rep*. 2012;5:1191-6.

15. Chen YJ, Wu H, Zhu JM, et al. MicroRNA-18a modulates P53 expression by targeting IRF2 in gastric cancer patients. *J Gastroenterol Hepatol*. 2016;31:155-63.

16. Chen YJ, Liang L, Li J, et al. IRF-2 Inhibits Gastric Cancer Invasion and Migration by Down-Regulating MMP-1. *Dig Dis Sci*. 2020;65:168-177.

17. Fornes O, Castro-Mondragon JA, Khan A, et al. JASPAR 2020: update of the open-access database of transcription factor binding profiles. *Nucleic Acids Res*. 2020;48:D87-D92.

18. Chen YJ, Li J, Lu N, Shen XZ. Interferon regulatory factors: A key to tumour immunity. *Int Immunopharmacol*. 2017;49:1-5.

19. Huff V. Wilms' tumours: about tumour suppressor genes, an oncogene and a chameleon gene. *Nat Rev Cancer*. 2011;11:111-21.

20. Fu C, Liang X, Cui W, et al. beta-Catenin in dendritic cells exerts opposite functions in cross-priming and maintenance of CD8+ T cells through regulation of IL-10. *Proc Natl Acad Sci U S A*. 2015;112:2823-8.

21. Spranger S, Gajewski TF. A new paradigm for tumor immune escape: beta-catenin-driven immune exclusion. *J Immunother Cancer*. 2015;3:43.

22. Pai SG, Carneiro BA, Mota JM, et al. Wnt/beta-catenin pathway: modulating anticancer immune response. *J Hematol Oncol*. 2017;10:101.

Table 1. Correlation between IRF-2 and clinicopathologic characteristics

	Total	IRF-2 expression		P value
		Low (35)	High (37)	
Sex				
Male	55	28 (50.9)	27 (49.1)	0.483
Female	17	7 (41.2)	10 (58.5)	
Age(y)				
< 60	34	16 (47.1)	18 (52.9)	0.803
≥ 60	38	19 (50.0)	19 (50.0)	
Invasive depth				
mucosa to muscularis propria	21	9 (42.9)	12 (60.6)	0.150
adventitia to adjacent structure	51	22 (56.4)	17 (43.6)	
Lymph nodes metastasis				
≤ 2 regions	33	13 (39.4)	20 (30.77)	0.407
> 2 regions	39	31 (60.78)	20 (39.22)	
Distant metastasis				
Yes	8	6 (75.0)	2 (25.0)	0.146
No	64	29 (45.3)	35 (54.7)	
Position				
Antrum and gastric angle	32	14 (43.8)	18 (56.3)	0.460
Others	40	21 (52.5)	19 (47.5)	
Size				
< 4cm	27	13 (48.1)	14 (51.9)	0.951
≥ 4cm	45	22 (48.9)	23 (51.1)	
TNM stage				
I, II	28	12 (42.9)	16 (57.1)	0.436
III, IV	44	23 (52.3)	21 (47.7)	

Note: Fisher's exact tests in distant metastasis; χ^2 test for all the other analyses.

Table 2. Univariate and multivariate analyses of factors associated with survival and cancer free survival

	OS		DFS	
	Hazard ratio (95%CI)	**P values**	**Hazard ratio (95%CI)**	**P values**
Univariate analyses				
Sex (male vs female)	0.875 (0.417, 1.836)	0.725	1.016 (0.484, 2.131)	0.967
Age, y (< 60 vs ≥ 60)	1.088 (0.800, 1.480)	0.589	1.050 (0.772, 1.427)	0.756
Invasive depth (mucosa to muscularis propria vs adventitia to adjacent structure)	0.434 (0.259, 0.728)	0.002	0.405 (0.241, 0.680)	0.001
Lymph nodes metastasis (≤ 2 regions vs > 2 regions)	0.432 (0.296, 0.629)	< 0.001	0.422 (0.289, 0.616)	< 0.001
Distant metastasis (yes vs no)	2.183 (0.912, 5.227)	0.080	2.514 (1.050, 6.018)	0.039
Position (antrum vs others)	0.965 (0.707, 1.318)	0.824	0.945 (0.693, 1.290)	0.723
TNM stage (I, II vs III, IV)	3.775 (1.735, 8.210)	0.001	3.947 (1.810, 8.607)	0.001
Size (< 4cm vs ≥ 4cm)	2.571 (1.256, 5.264)	0.010	2.505 (1.223, 5.131)	0.012
IRF-2 (positive vs negative)	2.913 (1.538, 5.518)	0.001	2.517 (1.337, 4.738)	0.004
Multivariate analyses				
IRF-2 (positive vs negative)	3.335 (1.736, 6.404)	< 0.001	2.756 (1.451, 5.234)	0.002
Size (< 4cm vs ≥ 4cm)	1.628 (0.760, 3.485)	0.209	1.544 (0.713, 3.347)	0.271
TNM stage (I, II vs III, IV)	3.495 (1.516, 8.058)	0.003	3.522 (1.509, 8.220)	0.004

Note: Cox proportional hazards regression model was used in univariate analysis. Multivariate analysis and Cox proportional hazards regression model were used in multivariate analysis. Variables were adopted for their prognostic significance by univariate analysis with forward stepwise selection (forward, likelihood ration). Variables were adopted for their prognostic significance by univariate analysis ($p<0.05$).

Abbreviations: 95%CI, 95% confidence interval.

Figure Legends

Fig. 1. Increase IRF-2 expression is related with favorable prognosis in GC patients. (A) The expression level of IRF-2 was examined in the tissue microarray containing 72 pairs of GC tissues and normal adjacent tissues by immunohistochemically analyses. (B) It was found that the expression level of IRF-2 was lower in GC tissues than in normal adjacent tissues. (C) The IRF-2 expression level was significantly correlated with patients' OS. (D) The IRF-2 expression level was significantly correlated with patients' DFS.

Fig. 2. IRF-2 can affect GC cells proliferation in vitro and in vivo. (A) Colony formation assays showed that colony formation ability was negative correlated with the expression of IRF-2. (B) EdU assays also showed that the GC cell proliferation ability was negative correlated with the expression of IRF-2. (C) In the xenograft tumor model, tumor volume increased in the IRF-2 knock down group.

Fig. 3. IRF-2 directly activate AMER1 transcription and regulate Wnt/β-catenin signaling pathway. (A) The peak information in ChIP-Seq analysis and proportion of IRF-2 binding to promoter regions. (B) Enrichment analysis of GO-Biological Precell with IRF-2 expression was shown. (C) KEGG analysis also showed that IRF-2 might affect several cancer pathways. (D) ChIP-Seq showed that IRF2 may act on the promoter region of AMER-1. (E) Possible binding sites of IRF-2 was found by JASPAR 2020 database. (F) It was found that there were two predicted IRF-2 binding sites in the AMER1 transcription start domain. (G) Luciferase assays for detecting

luciferase activity of AMER1-promoter-WT, AMER1-promoter-Mut1 and AMER1-promoter-Mut2 after IRF-2 overexpression.

Fig. 4. The expression level of AMER1 was positively related with IRF-2. (A & B) Western blotting and RT-PCT verified the positive relationship between IRF-2 and AMER1 in both protein and mRNA levels while Wnt/β-catenin signaling pathway was negatively correlated with the expression of IRF-2 and AMER1 in protein levels. (C) Immunohistochemical scores showed a positive correlation between AMER1 and IRF-2 in tissue microarray. (D) A positive correlation between AMER1 and IRF-2 was found in xenografted tumor tissues and a significant inverse correlation was also found between the expression of AMER1 and CD44. (E) A positive correlation was also found between the expression of IRF-2 and AMER1 on website GEPIA. $*P < 0.05$, $**P < 0.005$ and $***P < 0.0005$.

Fig. 5. IRF-2 inhibiting the Wnt/β-catenin signaling pathway depends on the regulation of AMER1. (A and D) Western blotting verified that the negative regulatory of IRF-2 on Wnt/β-catenin pathway was relied on AMER1. (B and E) Colony formation ability was increased when AMER1 was knocked down even if the IRF-2 was overexpressed and opposite result was found when AMER1 was over-expressed even if the IRF-2 was knocked down. (C and F) EdU assays also showed that the cell proliferation ability was depends on the regulation of AMER1.

Supplemental Fig.1. Signal mechanism of IRF-2 adversely affected the Wnt/β-catenin signaling pathway by regulating AMER1 expression.

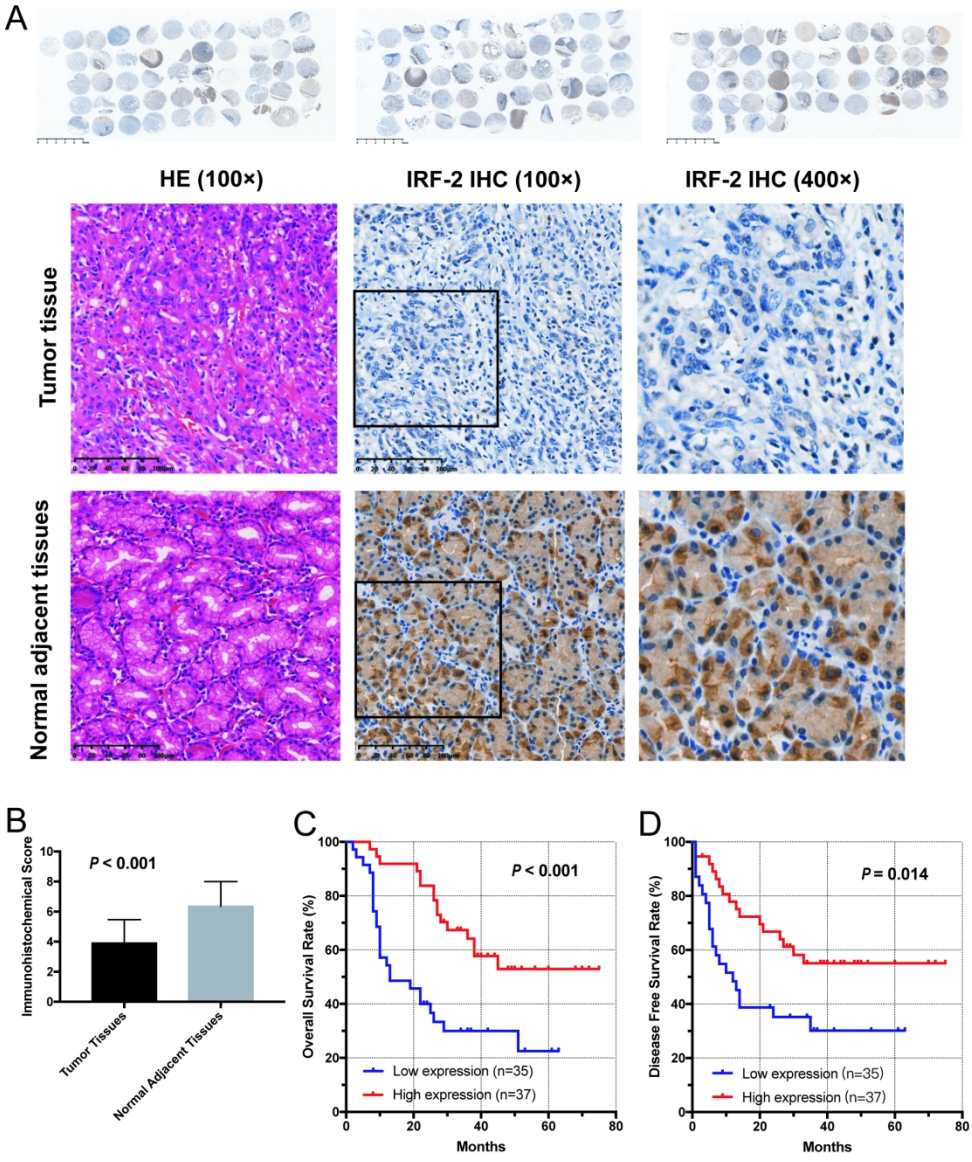

Fig. 1. Increase IRF-2 expression is related with favorable prognosis in GC patients. (A) The expression level of IRF-2 was examined in the tissue microarray containing 72 pairs of GC tissues and normal adjacent tissues by immunohistochemically analyses. (B) It was found that the expression level of IRF-2 was lower in GC tissues than in normal adjacent tissues. (C) The IRF-2 expression level was significantly correlated with patients' OS. (D) The IRF-2 expression level was significantly correlated with patients' DFS.

186x222mm (300 x 300 DPI)

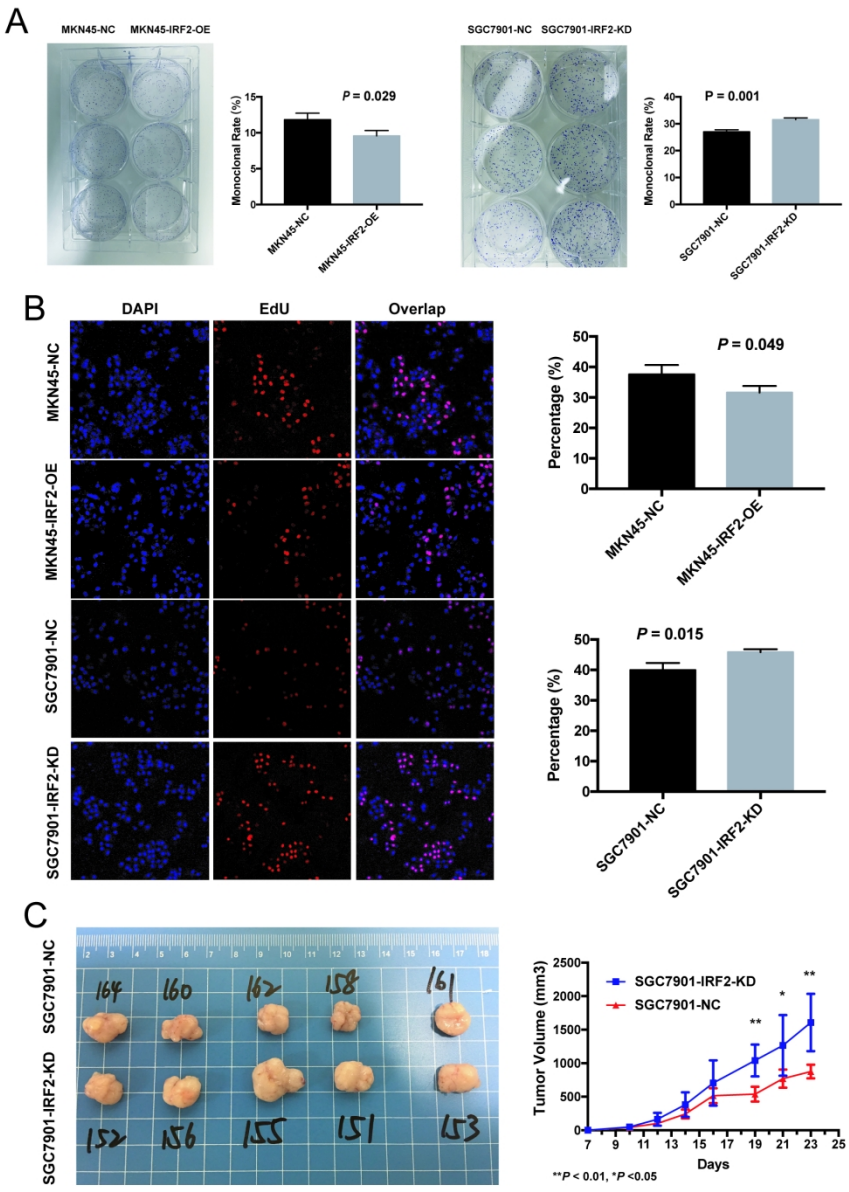

Fig. 2. IRF-2 can affect GC cells proliferation in vitro and in vivo. (A) Colony formation assays showed that colony formation ability was negative correlated with the expression of IRF-2. (B) EdU assays also showed that the GC cell proliferation ability was negative correlated with the expression of IRF-2. (C) In the xenograft tumor model, tumor volume increased in the IRF-2 knock down group.

160x218mm (300 x 300 DPI)

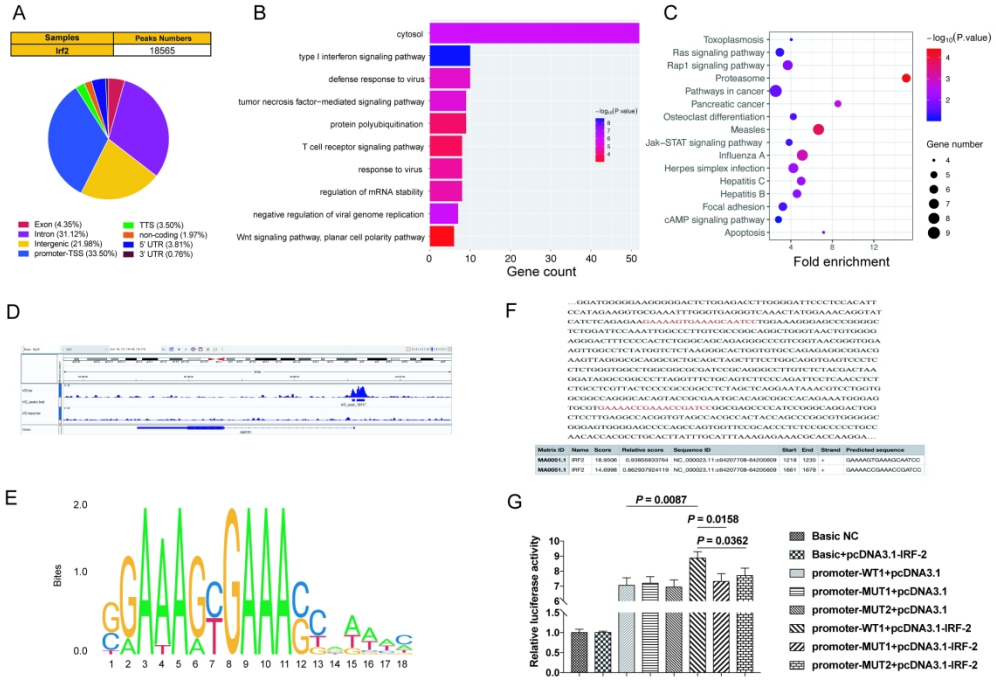

Fig. 3. IRF-2 directly activate AMER1 transcription and regulate Wnt/β-catenin signaling pathway. (A) The peak information in ChIP-Seq analysis and proportion of IRF-2 binding to promoter regions. (B) Enrichment analysis of GO-Biological Precell with IRF-2 expression was shown. (C) KEGG analysis also showed that IRF-2 might affect several cancer pathways. (D) ChIP-Seq showed that IRF2 may act on the promoter region of AMER-1. (E) Possible binding sites of IRF-2 was found by JASPAR 2020 database. (F) It was found that there were two predicted IRF-2 binding sites in the AMER1 transcription start domain. (G) Luciferase assays for detecting luciferase activity of AMER1-promoter-WT, AMER1-promoter-Mut1 and AMER1-promoter-Mut2 after IRF-2 overexpression.

210x150mm (300 x 300 DPI)

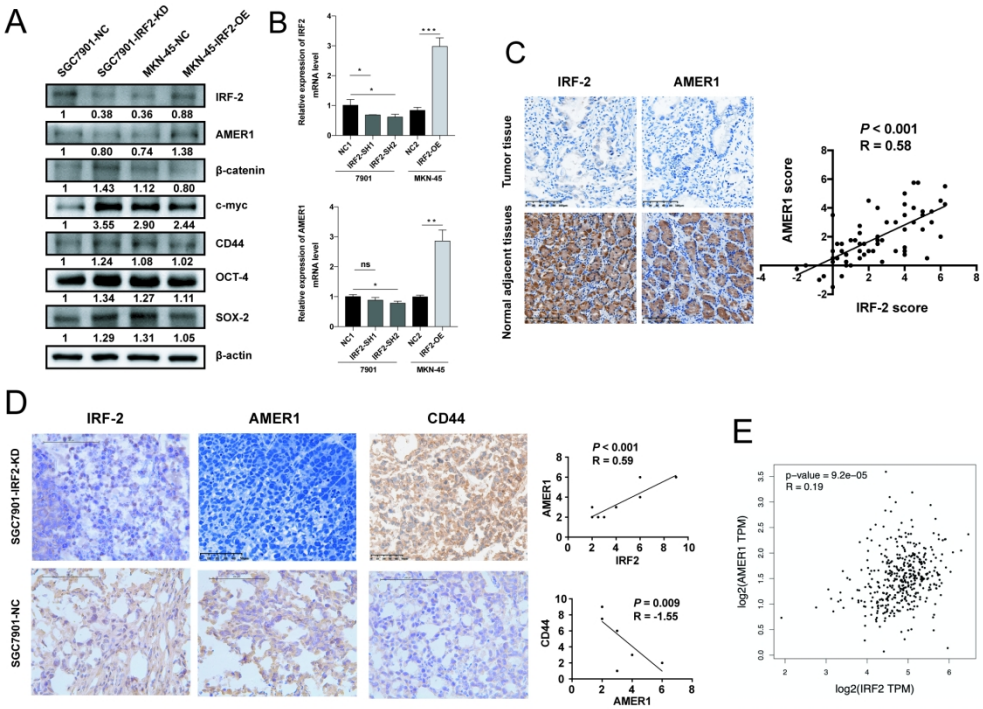

Fig. 4. The expression level of AMER1 was positively related with IRF-2. (A & B) Western blotting and RT-PCT verified the positive relationship between IRF-2 and AMER1 in both protein and mRNA levels while Wnt/β-catenin signaling pathway was negatively correlated with the expression of IRF-2 and AMER1 in protein levels. (C) Immunohistochemical scores showed a positive correlation between AMER1 and IRF-2 in tissue microarray. (D) A positive correlation between AMER1 and IRF-2 was found in xenografted tumor tissues and a significant inverse correlation was also found between the expression of AMER1 and CD44. (E) A positive correlation was also found between the expression of IRF-2 and AMER1 on website GEPIA. *P < 0.05, **P < 0.005 and ***P < 0.0005.

190x143mm (300 x 300 DPI)

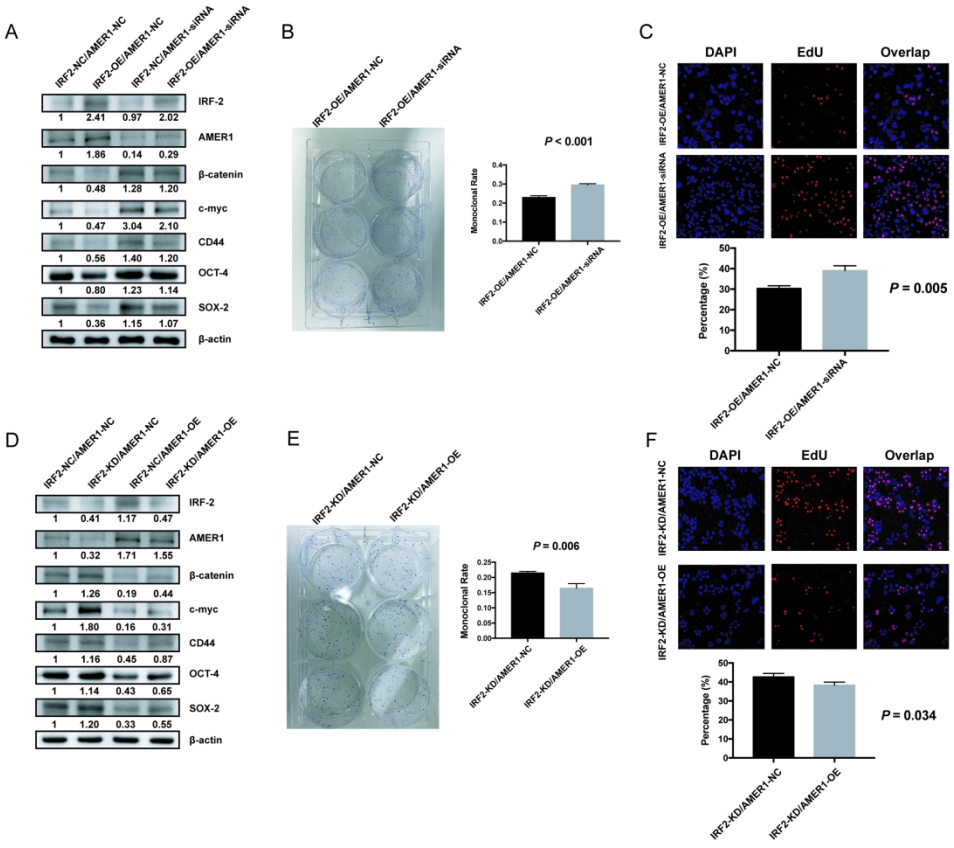

Fig. 5. IRF-2 inhibiting the Wnt/β-catenin signaling pathway depends on the regulation of AMER1. (A and D) Western blotting verified that the negative regulatory of IRF-2 on Wnt/β-catenin pathway was relied on AMER1. (B and E) Colony formation ability was increased when AMER1 was knocked down even if the IRF-2 was overexpressed and opposite result was found when AMER1 was over-expressed even if the IRF-2 was knocked down. (C and F) EdU assays also showed that the cell proliferation ability was depends on the regulation of AMER1.

210x178mm (300 x 300 DPI)

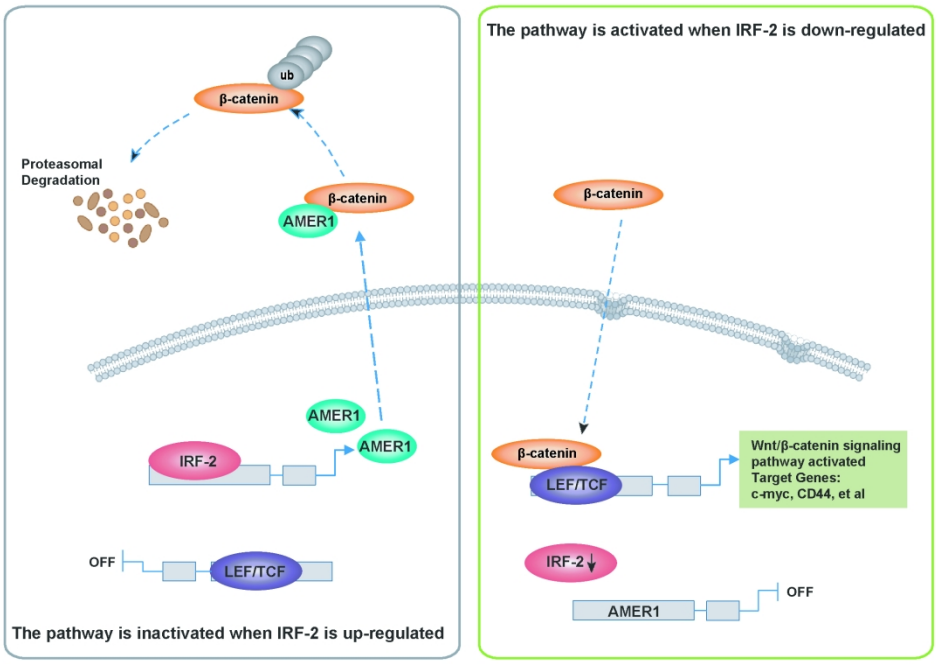

210x148mm (300 x 300 DPI)